Journal of Sedimentary Environments (2023) 8:491–505
https://doi.org/10.1007/s43217-023-00145-7

RESEARCH

Retrospective appurtenance of Euler and Werner deconvolution contiguity for source depth excogitation of Bouguer anomalies in the Benue Trough, Nigeria

A. J. Ilozobhie[1] · J. S. Ejepu[2] · A. Szafarczyk[3] · O. E. Agbasi[4] · N. J. Inyang[4,5] · D. I. Egu[6]

Received: 13 May 2023 / Revised: 9 July 2023 / Accepted: 15 July 2023 / Published online: 26 July 2023

Abstract

The leading cause of the glaring inexplicable errors in the accuracy of depth to anomaly assessments may be the technical challenge of the Euler deconvolution method from gravity surveys to perspicuously exhilarate the shape of major granitoid, tectonic lineaments, and local and regional fault systems without the existence of cogent correlative analytical simulation tools. That enigma becomes cumbersome with the increased existence of significantly incoherent density contrast between altered rocks or structures and their host rocks. That erudition aims to conduct a retrospective comparative analysis of the Euler and Werner deconvolution methods for effective depth excogitation of Bouguer anomalies in the Benue Trough, Nigeria. Comparing the previously acquired Werner deconvolution for deep and shallow source data to the detailed and comprehensive results of the Euler deconvolution gave the desired results. The study utilized various filtering techniques to analyze Bouguer anomalies and develop derivative grids to identify distinct subsurface features, such as sedimentary formations, alluvial deposit zones, and regions with high- and low-density rock minerals. Results of the comparative analysis of Euler and Werner deep source gave a minimum of 7.17 km for block 8 and a maximum of 19.8 km for block 15 for Euler. It gave a minimum of 6.89 km for block 9 and a maximum of 21.4 km for block 15. The deep source trend result gave a relatively stable deep source signal from blocks 1 to 9; while, there was inconsistency for blocks 10 and 11, then with a sudden increase in signal strength. This inconsistency is perhaps due to the complexity of the anomaly and inconsistency detected using both methods for depth resolution. Observations showed a similar trend for shallow source results. Suggestions showed that the region has potential for hydrocarbon and economic mineral exploration, making it attractive for further geologic studies. Future gravity simulators should have multiple deconvolution windows to improve modeling accuracy. That can have valuable implications for Nigeria's oil and gas industry and other regions with similar geological characteristics.

Keywords Bouguer anomalies · Deconvolution · Source depth analysis · Euler · Werner

Communicated by H. Chaves

✉ O. E. Agbasi
agbasi.okechukwu@gmail.com

[1] Department of Geology, University of Calabar, Calabar, Nigeria

[2] Department of Geology, Federal University of Technology, Minna, Nigeria

[3] Faculty of Environmental Engineering and Energy, Cracow University of Technology, Cracow, Poland

[4] Okna Geoservices Nigeria Limited, Eket, Nigeria

[5] Department of Geoscience, University of Uyo, Uyo, Nigeria

[6] Department of Petroleum Engineering, Madonna University, Enugu, Nigeria

1 Introduction

The gravity method is a geophysical survey technique used to measure the gravitational field and detect density variations by indicating the presence of different materials or structures. This method is valuable for creating maps and models of subsurface materials without drilling or excavation. The gravity survey can be performed on land or in the air, with the airborne method being advantageous in areas that are difficult to access, such as bodies of water (Olurin et al., 2015; Reid & Thurston, 2014; Wright, 1976). To obtain a more detailed understanding of these variations, geophysicists use various techniques to analyze the data. One such technique is the 3D analytic signal method, which enhances the anomalies and provides a clearer subsurface image. This

method is advantageous in identifying small features, such as faults and fractures that may not be visible in the raw data. Another technique is Werner deconvolution, which estimates the depth of the sources of gravity anomalies by removing the effects of the Earth's curvature from the data. This method is particularly useful in regions with complex geology and uneven topography. 3D Euler deconvolution is another popular technique for estimating the depth of gravity sources (Likkason, 2007; Stavrev, 1997). It uses the Euler homogeneity equation to determine the location and depth of the sources. This method is beneficial in identifying the depth of multiple sources spaced. Multiple Source Werner deconvolution is a more advanced technique that can estimate the depth and geometry of multiple sources with different shapes and sizes (Falconer, 1911; Naidu, 1968). This method combines the Werner and Euler deconvolution methods to provide a more accurate and detailed interpretation of the subsurface. The choice of technique depends on the subsurface variation's complexity and the study's specific objective. Combining of these techniques can obtain a more comprehensive understanding of the subsurface variations and provide insights into the geological processes that have shaped the Earth's crust (Kamba & Ahmed, 2017; Sawata et al., 2019).

Qualitative interpretation of gravity data involves identifying patterns and trends in the data to describe the underlying geological structures that cause the anomalies. The interpretation typically involves a visual data analysis to identify the anomalies' location, shape, and orientation and infer their geological significance. Identifying geological features corresponding to gravity anomalies can provide insights into the subsurface geological processes, such as faulting, folding, and magma intrusion. On the other hand, quantitative interpretations involve mathematical techniques to estimate the numerical values of the depths and dimensions of anomalous sources. These techniques typically involve the inversion of gravity data to derive a 3D model of the subsurface density distribution, from which the depth and geometry of the anomalous sources can be estimated (Biswas et al., 2017; Nicolas, 2009; Thompson, 1982).

The accuracy of the quantitative interpretation depends on the quality of the gravity data, the choice of the inversion algorithm, and the prior information used in the modeling process. The quantitative interpretation is particularly useful for resource exploration, as it provides estimates of the geologic contacts, lineaments, and dykes of potential mineral and hydrocarbon deposits.

The 3D Euler deconvolution technique is commonly used to estimate the depths to anomalies of causative bodies (Layade et al., 2020). This technique is based on the Euler homogeneity equation, which relates the depth, location, and size of a gravity source. By applying this equation to the gravity data, it is possible to estimate the depths of subsurface structures and geological features (Egu and Ilozobhie, 2020). The gravity method itself is based on two laws proposed by Sir Isaac Newton in 1867 (Hartman et al., 1971; Layade et al., 2015; Spector & Grant, 1970a, 1970b). The attraction between two bodies of known masses is described by the first law, sometimes referred to as the law of universal gravitation. The applied force and the rate at which a body's momentum changes are related by the second law sometimes referred to as the law of motion. These laws form the foundation of the gravity method and provide the theoretical framework for interpreting gravity data. The 3D Euler deconvolution technique is particularly useful in identifying the depth of multiple sources that are closely spaced. It can also be used to estimate the geometry of subsurface structures, such as faults and fractures, which can provide valuable information about the tectonic history of an area (Reid et al., 1990; Mickus and Hinojosa, 2001; Revees, 2005). The use of the 3D Euler deconvolution technique in gravity surveys has greatly improved our understanding of the subsurface variations and the geological processes that shape the Earth's crust. It has also enabled us to locate valuable mineral and energy resources and make informed decisions about land use and development (Adegoke & Layade, 2019; Ilozobhie & Egu, 2021; Obiora et al., 2018; Olowofela et al., 2013).

The main issue is that, qualitatively, the gravity data cannot be properly evaluated to outline, analyze, and identify certain significant subsurface characteristics revealed by survey findings that may link geologic formations and structures creating anomalies (Ngozi et al., 2019). Errors due to qualitative interpretation perhaps during data input, simulation runs, and modeling techniques of the gravity simulator are probably the technical bane of actual estimation and deciphering of depths to geologic formations and structure-yielding anomalies. The presence of more noticeable density differences between changed rocks or structures and their host rocks may make this problem more difficult (Ofoha et al., 2016). The inability of most gravity survey results using only the Euler deconvolution method to reflect the shape of major granitoid, tectonic lineaments, and local and regional fault systems, the nonexistence of effective correlative comparative analysis is perhaps the main reason for the numerous technical deficiencies in the quality of depth to anomaly evaluation. This problem constitutes compounding errors of uncertainties for the basin experts for petroleum geology, sedimentology, mineralogy, petrology, mining, and petroleum engineers (Oghuma et al., 2015).

This study aims to carry out a retrospective comparative analysis of the Euler and Werner deconvolution for effective depth excogitation of Bouguer anomalies in the middle

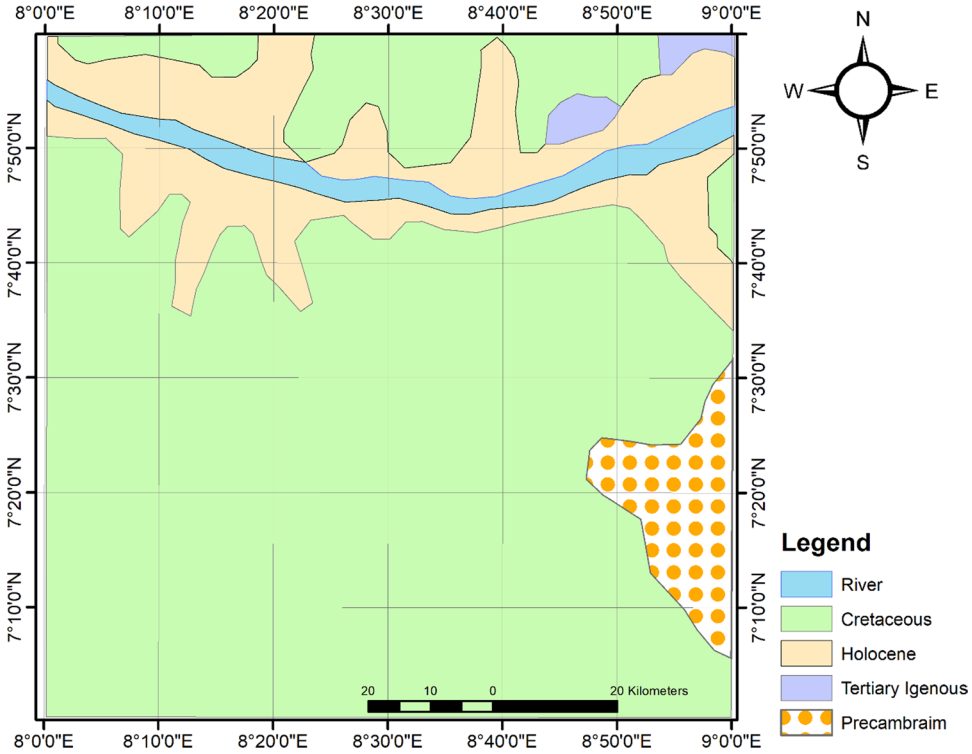

Fig. 1 Geologic map of the study area

Benue trough, Nigeria. This is achieved by comparing the previously acquired Werner deconvolution deep and shallow source data to the detailed and comprehensive results of the Euler deconvolution. This astute evaluation is essential to reducing errors due to avoidable uncertainties and discrepancies in deconvolution techniques. The accurate determination of depth to the source of anomalies detected in gravity data is crucial in geological exploration and resource exploitation. Bouguer anomalies are commonly used in geophysical surveys to identify areas with anomalous variations in gravity (Nabighian, 1972; Telford et al., 1990). However, the interpretation of these anomalies can be challenging due to their complex nature and the uncertainty associated with their source depths. This study will provide insights into the subsurface geological structures and contribute to the development of effective exploration strategies for mineral and hydrocarbon resources in the region.

2 Geology of the study area

The study area lies between latitude 7.00°N and 8.00°N, and longitude 8.00°E and 9.00°E within the middle Benue Trough. The middle Benue Trough is a linear terrain that is mostly flat or mildly undulating. Albian rocks that produced the Keana Anticline can be seen there. The Kadarko Basin to the north and the Wukari Basin to the south, both of which exhibit minor deformations, surround the region. The Benue Trough's other regions are divided from the Abakaliki area by the "Gboko Line." (Ofoegbu, 1983; Benkhelil, 1989).

The Asu River Group, largely made of green silty shales with occasional siltstones and fine-grained sandstones, represents the Albian stage within the middle Benue Trough. It is surrounded by the Awe Formation. The fossiliferous marine series of the Turonian era are widespread in the Benue Trough. The Turonian stage is represented in the middle Benue regions by the Eze Aku Formation, which is made up of hard, gray and black calcareous shale, limestone, and siltstone. Sandstone can change from shale in some places. The bluish-gray Awgu Shale, which is composed of fine-grained carbonaceous limestone layers and occasionally contains Agbani Sandstones, lies on top of the Eze Aku Formation(Igwe & Okoro, 2016). Ammonites from the Turonian period may be found in the formation's bottom portion, which corresponds to the early Coniacian stage. The dips of these structures usually do not exceed 30° and mostly run parallel to the Trough border in a northeast-to-southwest direction (Anudu et al., 2014). The sinistral migration along NE–SW shear zones is evident from the echelon arrangement of the fold axes caused by this deformation.

During the Palaeocene epoch, volcanic activity occurred in the middle Benue Trough, resulting in the emplacement of basic to intermediate volcanic rocks within the sedimentary layers. These volcanic rocks include basalts, phonolites, and trachytes and are found in the form of small cones, plugs, lava sheets, and tuffs, with limited distribution throughout

the region. The Awe, Arufu, and Makurdi areas have the most significant concentration of these volcanic rocks (Umukoro & Akanbi, 2014). In addition, the Makurdi area has Turonian shales and sandstones, while Oturkpo has shales that contain basaltic lava and dolerite sills in alternating layers. The surface geology of the research area is depicted in Fig. 1. Due to numerous tectonic and volcanic events, the geology of the study region is complex and features a diverse range of rock formations and properties.

Multiple studies, such as Nwosu (2014), Umukoro and Akanbi (2014), Oghuma et al. (2015), and Layade et al. (2015), have reported that the study area consists of various types of rocks, including crystalline basement rocks, younger granites, sedimentary rocks, and volcanic rocks. Specifically, the northern and southern regions of the parts are underlain by crystalline basement rocks, which belong to the Northern Nigerian Basement Complex and the Eastern Nigerian Basement Complex, respectively. The Migmatite–Gneiss Complex and the Older Granites are two groups of these crystalline basement rocks, also referred to as Pan-African Granitoids.

The Migmatite–Gneiss Complex, which comprises migmatites, gneisses, and schists, ranges in age from the Mesoarchaean to the Neoproterozoic, spanning from 3200 million years ago (Ma) to 542 Ma. The Older Granites, on the other hand, are Pan-African and date back to the Neoproterozoic to Early Paleozoic era, spanning from 600 to 200 Ma (Van-breemen et al., 1977). These granitoids comprise of granites, diorites, and dolerites. During the Pan-African tectonic events, which occurred from 600 to 200 Ma, the earlier granites invaded and distorted the Migmatite–Gneiss Complex (Hesham & Hesham, 2016). In the northwest region of the study area are the Mada and Afu ring complexes, which are younger, high-level anorogenic granites that range in age from 210 to 145 Ma, corresponding to the Triassic–Jurassic era (Hesham & Hesham, 2016). These younger granites consist mainly of microgranites and biotite granites and are found near the margin of the trough (Hansen & Simmonds, 1993; Phillips et al., 1998).

3 Methodology

The Bureau Gravimetrique Internationale (BGI) provided the gravity statistics for the study area, which were used to generate the Bouguer anomaly map. The map was initially created using the Universal Transverse Mercator (UTM) Zone 32 Northing projection and was later reprojected to UTM Zone 31 Northing. To identify the deep, middle, and shallow anomalous gravity sources in the study area, two-dimensional fast Fourier transform (FFT2D) filter within the MAGMAP, module of Oasis Montaj (version 8.4) software, was applied to the Bouguer anomaly grid. (Reford & Summer, 1964). The obtained Radially Average Power Spectrum (RAPS) enabled appropriate visualization of the depth-dependent responses of the gravity field. Each segment represents the gravity response at different depths. The slope of the line segment is proportional to the depth. To enhance the shallow signals in the residual anomaly map, a high-pass filter was applied, and a Regional-Residual separation method was employed. To create residual maps of the first, second, third, and other higher degrees, the polynomial trend technique was used in the Regional-Residual separation process. The intricacy of the local geology influences this polynomial's order to some extent. The Bouguer anomaly map was used to guide the polynomial surfaces in accordance with an algorithm created by Spector and Grant in 1970. The analytical least squares approach and the polynomial decomposition series are both used in this algorithm. The residual was created by deducting the regional field from the gravitational field that was actually measured. The cut-off wave number was set to 0.02 cycles/km, and the intermediate and shallow sources were processed as the residual anomaly, which was derived from the Bouguer gravity field. This approach was reported in previous studies by Whitehead and Musselman (2005) and Reid et al. (2014).

Once the residual anomaly map was obtained, a derivative was taken along the X-axis to illustrate the variation of the gravitational anomaly for horizontal distance. An analytic signal map was also generated to identify the boundaries of anomalous sources and geological constraints. Despite its high noise level, the analytic signal map was extended 1 km uphill to improve its clarity. Additionally, a two-dimensional fast Fourier transform (FFT2D) was employed to emphasize features associated with shallow causes (Rivas, 2009; Roest et al., 1992; Zahra and Oweis, 2016).

To locate the gravity source, the 3D Euler deconvolution method was utilized, which relies on homogeneity equations that connect the gradient components of the potential field to the source location. The degree of the structural complexity of the gravity sources is quantified using the structural index (SI) η, which can range from 0 to 2. Various theoretical shapes of gravity sources are associated with different SI values, including a sphere with $\eta = 2$, a vertical line termination (pipe) with $\eta = 1$, a horizontal line (cylinder) with $\eta = 1$, a thin bed fault with $\eta = 1$, and a thin sheet edge with $\eta = 0$.

The shape and position of the gravity sources may be determined, and it offers a helpful framework for investigating gravity anomalies. Equation 1 defines the 3D Standard Euler equation for the potential field.

$$X\frac{dT}{dx} + Y\frac{dT}{dx} + Z\frac{dT}{dz} + \eta T = X_0\frac{dT}{dx} + Y_o\frac{dT}{dy} + Z_o\frac{dT}{dz} + \eta b \tag{1}$$

The base level is b, and the measurement point contains coordinates of x, y, and z. The coordinates X_0, Y_o, and

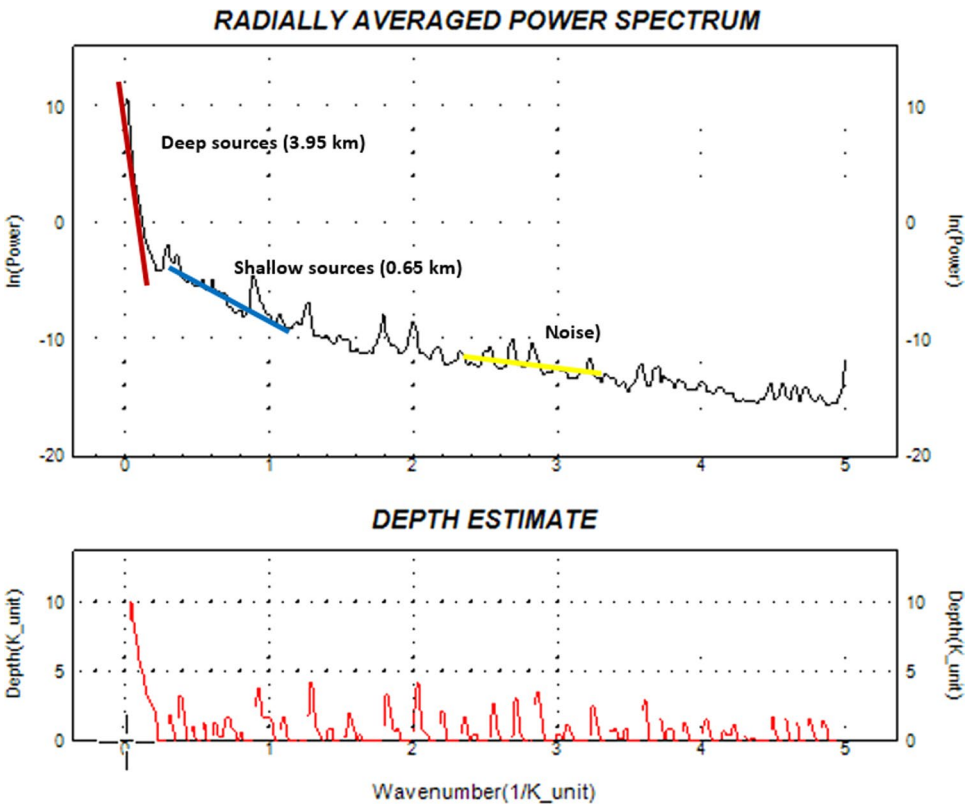

Fig. 2 Cut-off wave number and intermediate/shallow sources in the residual anomaly from Bouguer gravity field

Z_o, identify the source location, while T denotes the total potential field. Several structural indices of 0, 1, and 2 were investigated to compute the standard Euler deconvolution solutions, but only SI equal to 1 produced a geologically significant result. This shows that features like faults, contacts, and thin sheet edges may be present in the region (dikes). A 3000 by 3000 m square window was employed, and it includes several grid cells from the gridded dataset. A lower size would not have given enough information on the sources' depth while using a bigger window size would have resulted in a loss of spatial resolution.

4 Werner deconvolution technique

The expression for a dike's equation, which may be expressed as follows, make up the core theoretical equations of the Werner deconvolution technique:

$$F(x) = \frac{A(x - x_o) + B_z}{(x - x_o)^2 + z^2}, \tag{2}$$

where F stands for the total magnetic field intensity at location x, which is the length of a profile that crosses a dike. The distance horizontally along the profile from the point just above the top of the dike to its depth (z) is x_o. The variables A and B depend on the direction and magnetization of the dike. A, B, x_o, and z is the four unknown values that need to be determined.

Werner emphasizes that the equation may be rearranged into a particular form in a simple case where observations are made in a level plane across infinitely long and deep-level bodies with a striking perpendicular to the profile's direction.

$$x^2F(x) = a_0 + a_1x + b_0F(x) + b_1xF(x), \tag{3}$$

where $a_0 = -Ax_0 + Bz$, $a_1 = A$, $b_0 = -x_0^2 - z^2$ and $b_1 = 2x_0$.

By evaluating all four field points at once, a system of equations may be constructed to determine values for a_0, a_1, b_0, and b_1. These numbers enable the equation to be solved for x_0, z, A, and B.

The depth and position of the dike's top are related to the equation's parameters, on the other hand.

$$x_0 = \frac{1}{2}b_1 \text{ and } z = \pm\sqrt{-4b_0 - b_1^2}. \tag{4}$$

When there are four unknowns, a_0, a_1, b_0, and b_1 may be found by simultaneously solving equations for the four x values and their associated F values. From there, x_0 and z can be computed. This geometric solution is sufficient to ascertain the depth to the top of the dike or thin sheet in simpler situations.

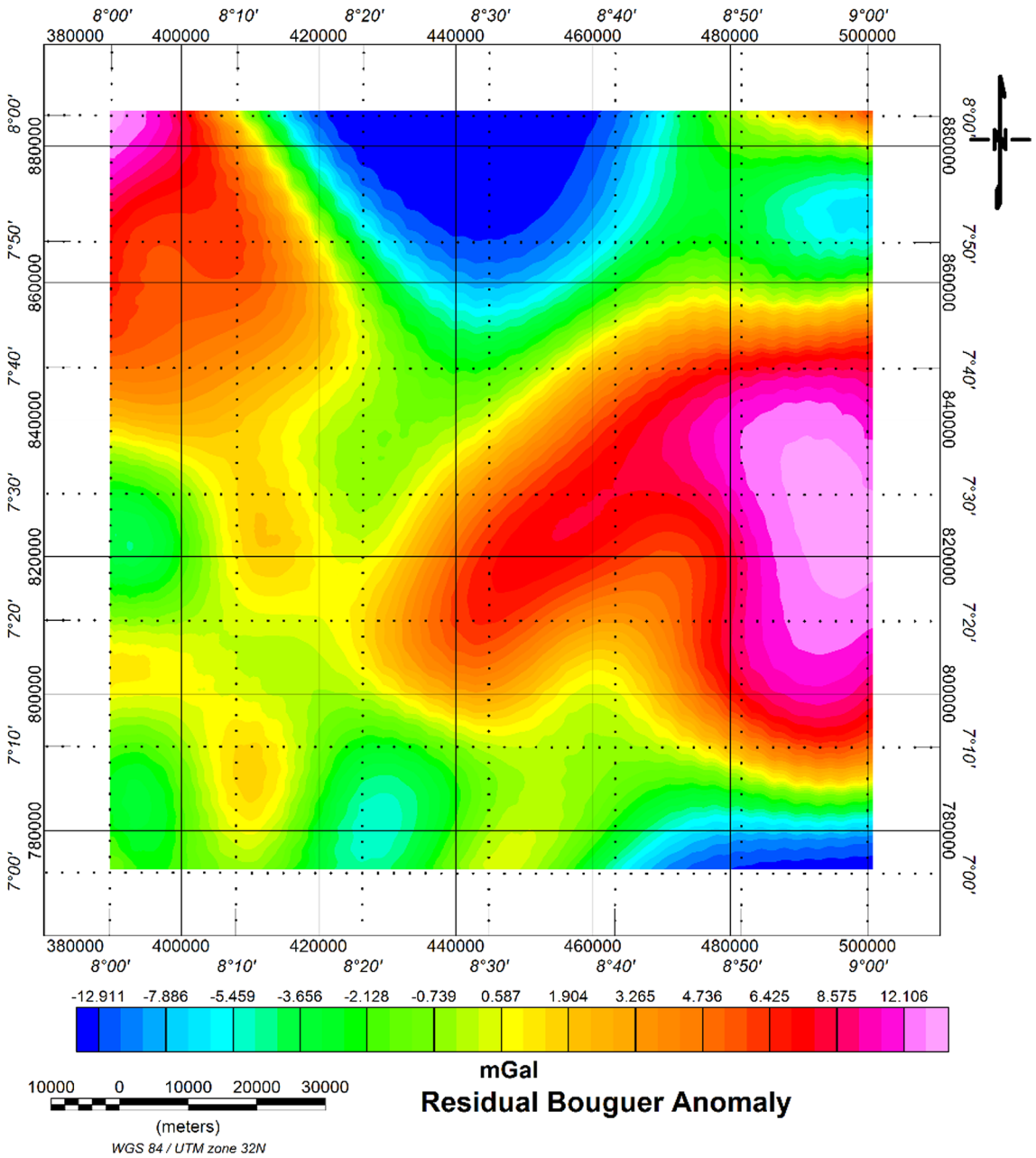

Fig. 3 Residual Bouguer anomaly map of the study area

However, adding an interference term in the form of a polynomial $C_0 + C_1x + C_2x^2 + \cdots + C_nx^n$ to the magnetic anomaly, the equation can increase the precision of the estimated physical quantities x_0, z, A, and B when interference is a possibility and can be represented by a polynomial to a certain degree.

$$F(x) = \frac{A(x - x_o) + B_z}{(x - x_o)^2 + z^2} + C_0 + C_1x + C_2x^2 + \cdots + C_nx^n. \tag{5}$$

The coefficients of an interference polynomial are denoted by Cs, and the polynomial's order is n. Since there are (n + 5) unknowns, it takes (n + 5) points to get the answers.

Source bodies can be divided into two categories for straightforward interpretation. Body types belonging to the first category have a depth from the observation plane that is about equal to their breadth. Since it is difficult to pinpoint their boundaries with any degree of certainty, these are known as thin bodies. The second category consists of entities with a significant amount of lateral extension and distinct edges. For the total magnetic field produced by thin

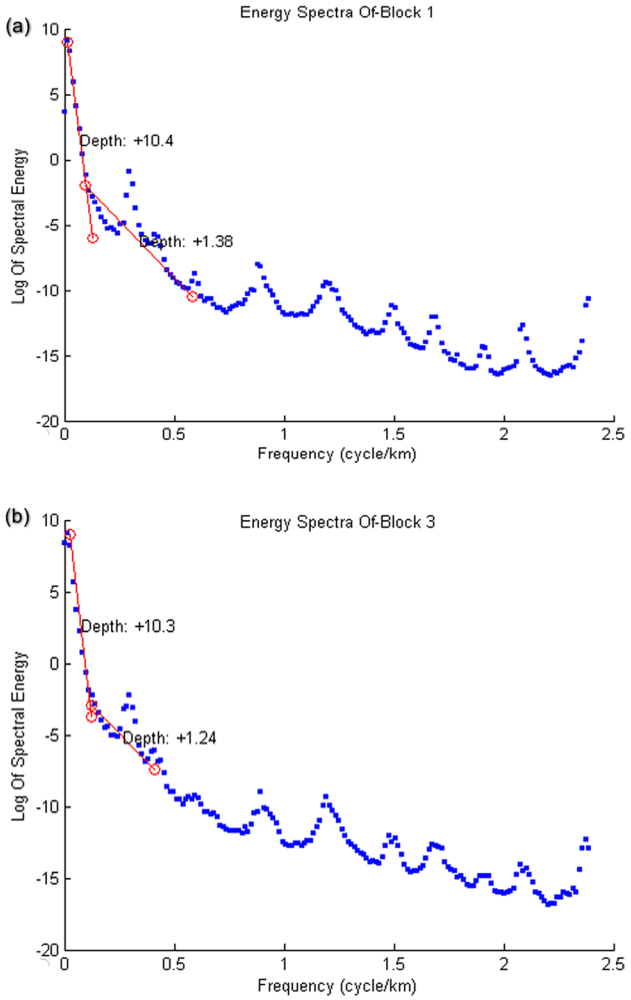

Fig. 4 Energy spectra for Blocks 1 (**a**) and 3 (**b**)

dikes with any dip, Werner (1953) offered an equation, and Hartman et al. (1971) replicated Werner's interpretation of the equations.

The Werner deconvolution operator is used as a moving window in the Werner deconvolution analysis to continuously solve for four unknowns along a profile. The window size, which influences the estimated depth of the anomaly; its movement on the profile, which impacts the number of solutions produced; and other characteristics that weed out noise-induced spurious solutions are among the operator's parameters. These features of the methodology were explained by Megwara and Udensi (2014). Basement rocks often have higher magnetic susceptibilities than sedimentary rocks. Therefore, variations in magnetic strength over basement complexes might be caused by the sedimentary structure, volcanic bodies within the basement or basin, or modifications in the susceptibilities of the materials inside the basement itself (Behrendt and Klitgord, 1980). As a result, one potential use for basement complexes is to utilize magnetic data to determine the depth of a magnetic source Fig. 2

5 Results and discussion

5.1 Qualitative treatment

The results of the regional Bouguer anomaly gave a range of − 27.688mgal from the northwest and increased diagonally in the south-eastern direction to approximately a maximum of 6.155mgal as shown in Fig. 3. Areal overview estimate shows that the study environment is about 80.37% embedded with negative gravity anomalies.

The residual map for the separated Bouguer anomaly grid is shown in Fig. 3. This map reveals the variations in the gravity field that are not accounted for by the expected gravity field due to the earth's shape and rotation. Results of the residual Bouguer anomaly map gave a range from a minimum of − 12.911 mgal in the northern and south-eastern regions and a maximum of 12.106 mgal in the eastern region. Across the study area, there is an even distribution of both negative and positive anomalies. However, there are more concentrated signals of negative anomalies ranging from − 3.656 mgal to − 0.739 mgal. On the other hand, the least negative anomaly is found in fewer locations and is sparsely distributed throughout the study area.

Gravity readings in the Bouguer anomaly field, range from − 27.688 mGal to 6.155 mGal. The anomaly map shows greater gravimetric values in the area's southeast, which is consistent with lithological changes below ground. On the other hand, the area's lithology's intra-basement showed poor gravimetric values in the northern, southwestern, and northwestern parts. When compared to the geological map of the research area, the predominance of high gravity values in the southeast suggests a potential undifferentiated gneiss complex, which is mostly composed of schist in the Gboko, Konshish, and Ushongo regions.

Results of energy spectra for blocks 1 and 3 for the gravity signal frequency (cycle/km) gave a declining gravitational spectral energy from + 10 to − 15 at a frequency of approximately 2.3 cycle/km as shown in Fig. 4a. Depth profiles of + 10.4 and + 1.38 were also predicted indicating the magnitudes of deep and shallow depth sources. Results of spectral energy with frequency profile for block 3 gave a similar declining trend of gravitational energy, but the depth profiles gave + 10.3 and + 1.24 as shown in Fig. 4b. The anomaly was filtered to reveal characteristics linked to intermediate and shorter wavelengths. This implies that the data were processed in a way that enhanced the features in the anomaly that correspond to wavelengths of intermediate and shorter lengths.

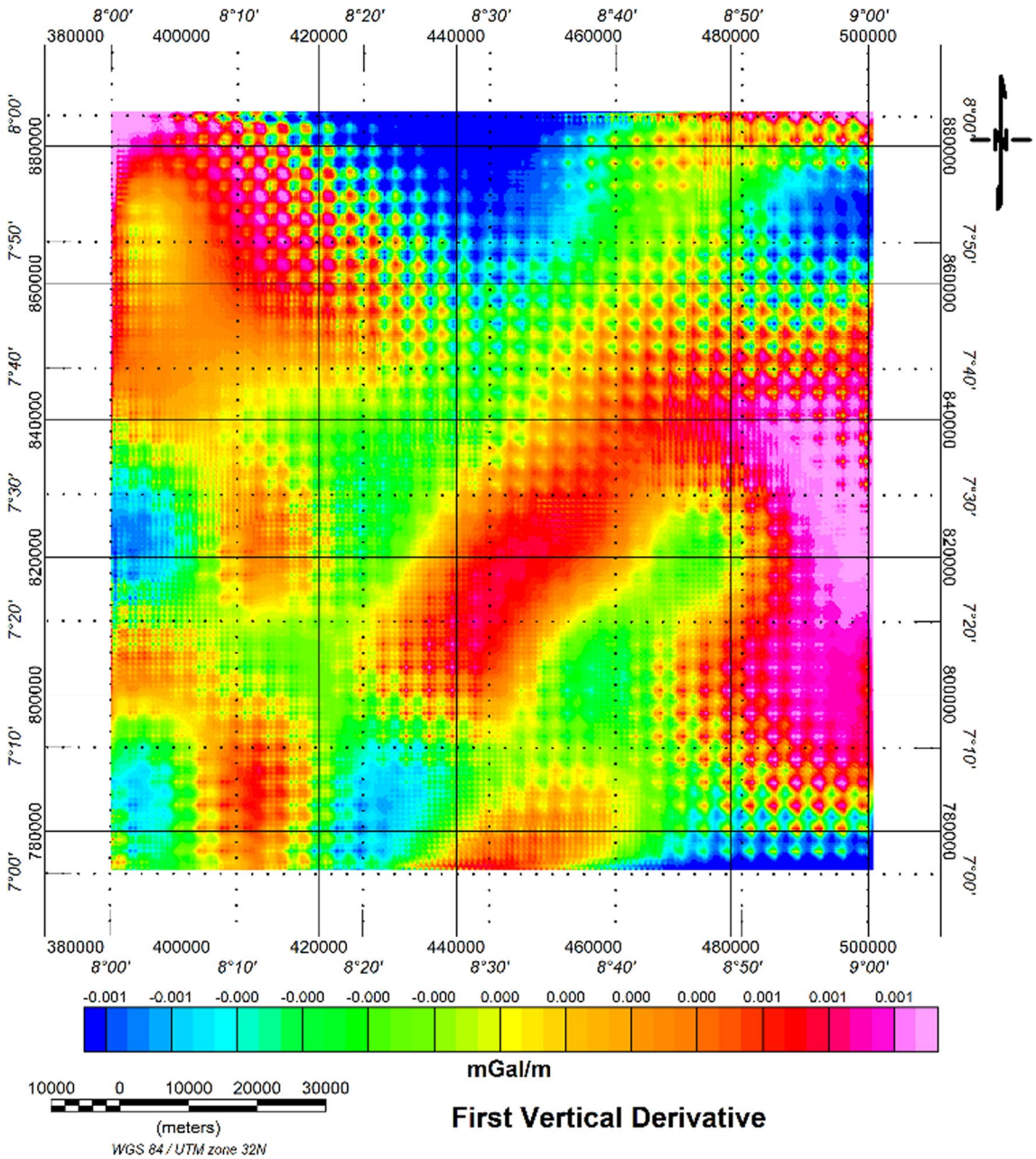

Fig. 5 First vertical derivative map of the study area

The residual anomaly grid was also processed to produce the First vertical derivative along the X-direction. Results of the first vertical derivative gave a range from a minimum of − 0.001 mgal/m. This appears to be sparsely located in the north-central and south-eastern regions, while + 0.001 mgal/m is densely located in the region as shown in Fig. 5.

The results of the analytical signal gave a range from -0.0 to a maximum of 0.001 mgal/m. This is densely located across the study area as shown in Fig. 5.

However, the analytic signal map was observed to have some noise, so it was further processed by extending its upward to a height of 1 km. Results of upward continuation at 1 km analytic signal gave a range from a minimum of − 32.002 mgal to a maximum of 10.879 mgal as shown in Fig. 6. The least gravitational signal of − 32.002 mgal is located in the north-central while the maximum signal is largely concentrated in the southeast.

This result was obtained to enhance the clarity of the anomalous sources and geological boundaries in the data.

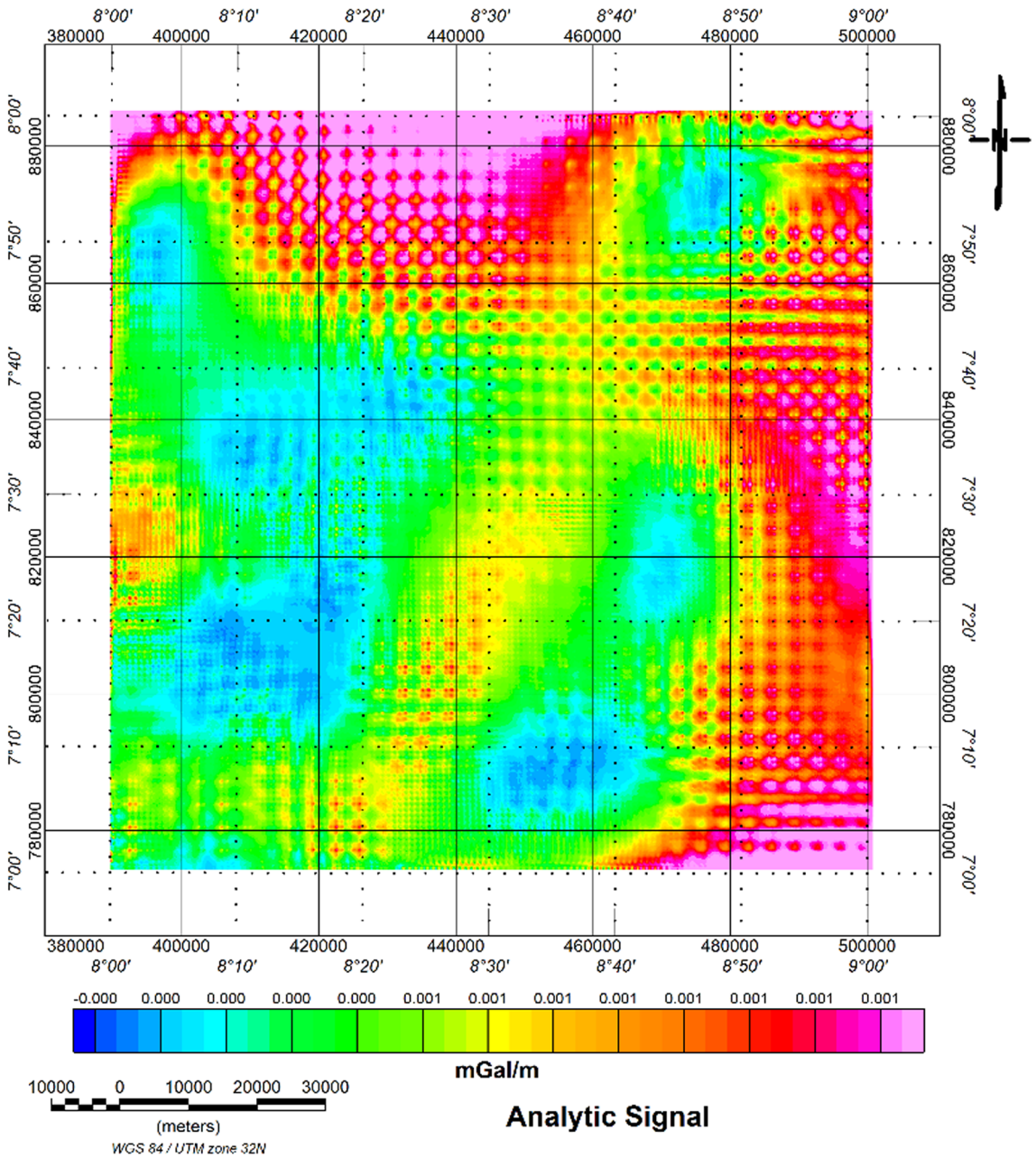

Fig. 6 Analytic signal map of the study area

The 3D standard Euler equation was utilized to compute the structural index (SI) values ranging from 0 to 2 for gravity sources. The SI values provided insight into the possible geometries of various theoretical structures, including spheres, vertical line ends (pipes), horizontal lines (cylinders), thin bed faults, and thin sheet edges Fig. 7

However, it was observed that only SI = 1 gave outputs with geologically important outcomes. According to Ikeh et al., (2017); Nwogwugwu et al., (2017) and Abdullahi et al., (2019), the region may be identified by characteristics including faults, contacts, and thin sheet edges (dikes).

Results of the Euler depth solution gave a depth range from − 5607.391 m to a maximum of − 185.004 m as shown in Fig. 8. These depths are closely packed together in the northwest, northeast, southwest, and southeast regions of the study area. It also gave a minimum of 7.17 km for block 8 to a maximum of 19.8 km for block 15 for the deep source

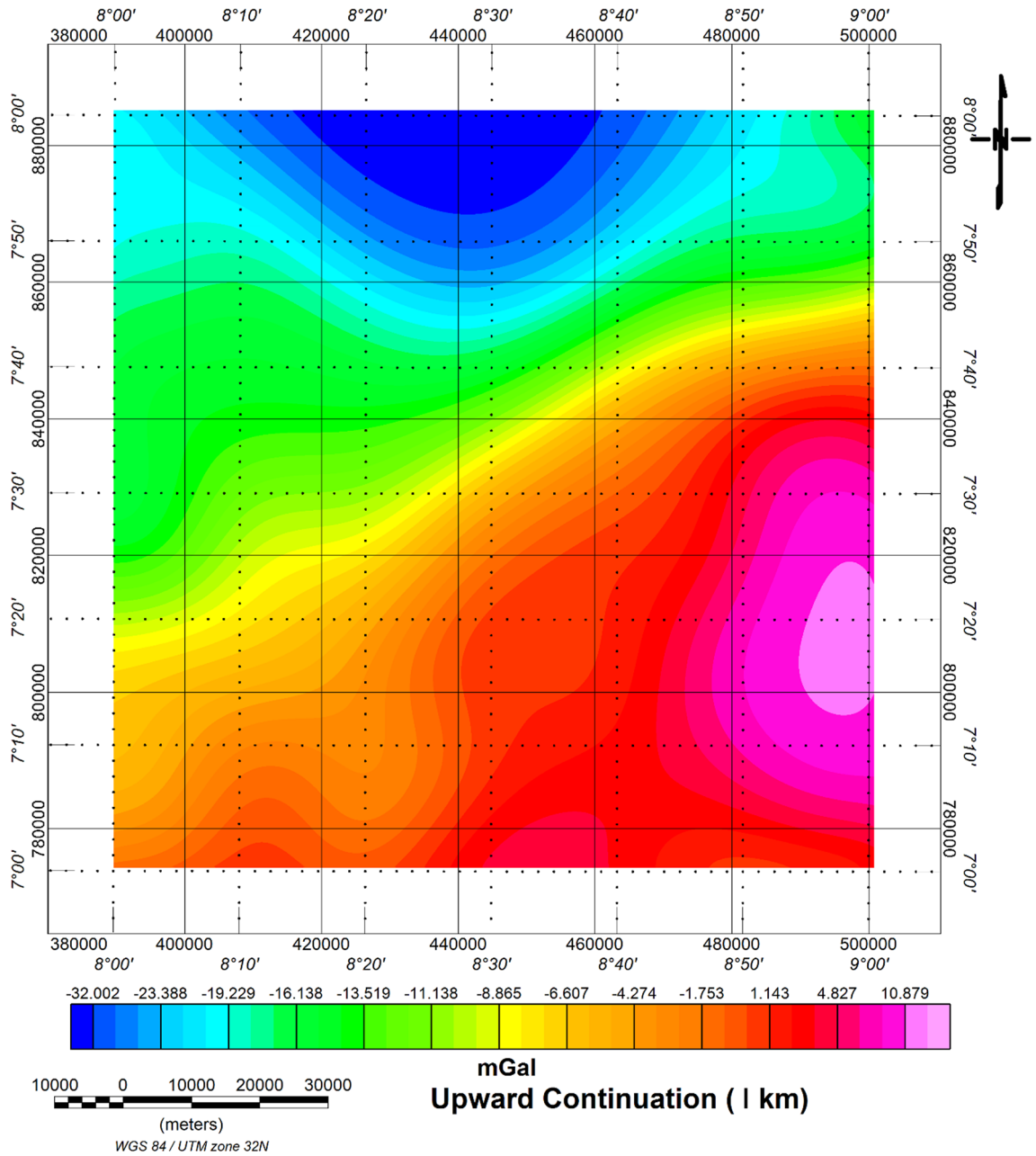

Fig. 7 Upward continuation to 1 km of analytic signal map of the study area

as shown in Table 1. It also gave a minimum of 1.16 km for block 13 to a maximum of 3.05 km for block 7 for the shallow source. It was observed that the depth range of 1,000–2,000 m densely populated the entire regions of the study area Fig. 9

This outcome displays an inferred lineament map of geological structures, confirming the presence of geological features like faults, dikes, and/or sills in the study region. The results support the hypothesis that the basement gravity anomalies examined in this study offer a trustworthy representation of the sedimentary thickness (Epuh et al., 2020). Further geological research and exploration efforts in the area will benefit from these discoveries, which also point to opportunities for hydrocarbon exploration and economic mineral exploration (including barite, cadmium, coal, copper, gypsum, lead, silver, and zinc) (Emujakporue et al., 2018).

Euler technique results showed variations in density contrast of the underlying geological features in the study region. The geological formations in the area and their

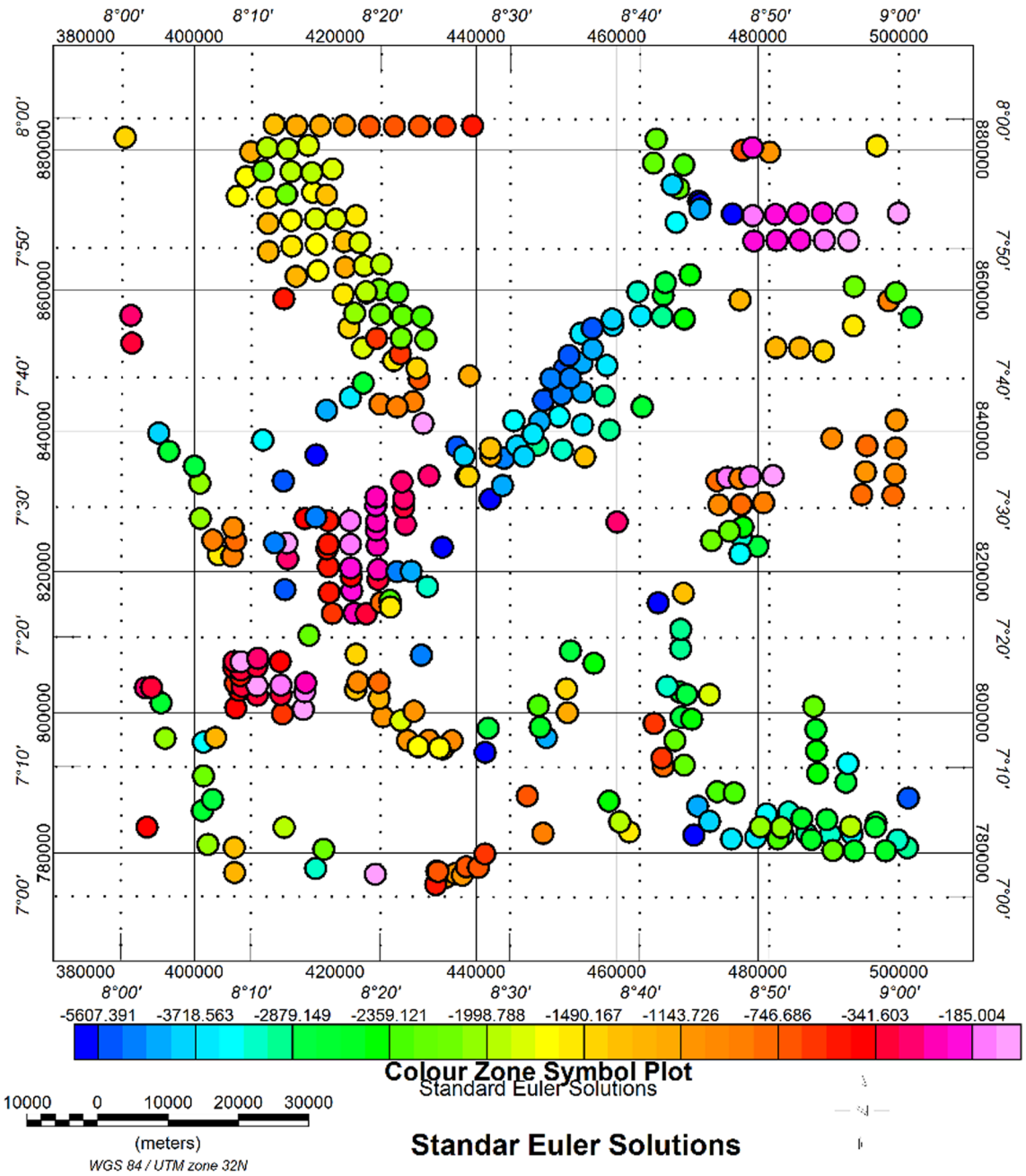

Fig. 8 Euler depth solutions for the study area

potential for natural resource exploitation can be better understood with the use of this knowledge.

Comparative results of the Euler and Werner deconvolution analysis were done using the deep and shallow source depths (km). Results of the comparative analysis of Euler and Werner deep source gave a minimum of 2.79 km for block 12 and a maximum of 5.83 km for block 9 for Euler. It gave a minimum of 3.89 km for block 9 and a maximum of 8.37 km for block 2 as shown in Table 2. The deep source trend result show a relatively stable deep source signal from Blocks 3 to 8 while there was inconsistency for Blocks 1 and 2, then with a sudden increase in signal strength. This inconsistency is perhaps due to the complexity of the anomaly and inconsistency detected using both methods of deconvolution for depth resolution.

Comparative results for shallow source signals of the Euler and Werner gave a declining trend of shallow source signals from blocks 1 to 15 as shown in Table 2. The

Table 1 Euler depth solution for the study area

Block	Deep Source (km)	Shallow source (km)
1	5.74	0.363
2	3.53	0.332
3	4.41	0.432
4	4.19	0.353
5	4.37	0.263
6	3.87	0.35
7	4.06	0.462
8	3.94	0.399
9	5.83	0.458
10	5.45	0.472
11	4.54	0.351
12	2.79	0.402
13	3.9	0.644
14	4.26	0.395
15	4.45	0.65

discrepancy was, however, observed at blocks 3, 6, 7, and 15 which also confirms the concerns of the authors for the need to seriously consider the application of at least two deconvolution techniques for validating and ensuring improved quality of result obtained from gravity anomaly depth signal sources.

The results obtained from the study of the area suggest that there are promising prospects for hydrocarbon exploration based on the depths of the basement gravity sources. The findings also indicate that the area has the potential for the exploration of valuable economic minerals. This information could be extremely valuable for further geological studies and exploration activities in the region. With this knowledge, researchers and exploration companies can focus their efforts and resources on areas with the highest potential for successful exploration and exploitation. The economic benefits of these activities could be significant, not just for the local area, but for the wider economy as well. These findings also contribute to the understanding of the geology of the region, which could have implications for other fields such as environmental management and disaster risk reduction.

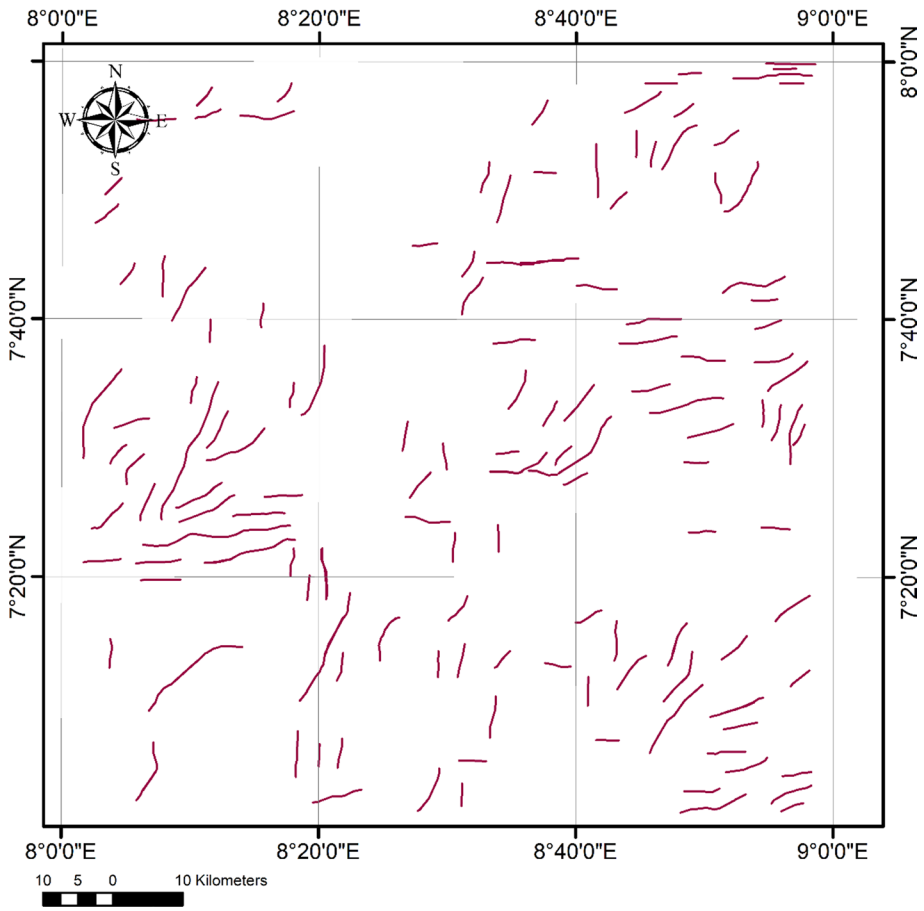

Fig. 9 Lineamnet map of the study area

Table 2 Euler and Werner deep source for the study area

Blocks	Euler deep source (km)	Werner deep source (km)	Euler shallow source (km)	Werner shallow source (km)
1	5.74	7.26	0.363	1.02
2	3.53	8.37	0.332	0.82
3	4.41	8.25	0.432	0.91
4	4.19	6.47	0.353	1.59
5	4.37	7.19	0.263	1.25
6	3.87	6.34	0.35	1.76
7	4.06	7.07	0.462	1.86
8	3.94	4.03	0.399	0.98
9	5.83	3.89	0.458	0.86
10	5.45	6.23	0.472	0.74
11	4.54	6.06	0.351	1.65
12	2.79	5.65	0.402	0.93
13	3.90	7.03	0.644	0.86
14	4.26	5.42	0.395	0.78
15	4.45	7.14	0.650	0.74

6 Conclusion

The gravity method is a geophysical survey technique used to measure the gravitational field and detect density variations by indicating the presence of different materials or structures In hindsight, this study aims to assess how well Euler and Werner's deconvolution techniques work to estimate the depth of Bouguer anomalies in the middle Benue trough, Nigeria. Precise anomaly source depth determination is essential for geological investigation and resource development. Due to their complexity and ambiguous source depths, Bouguer anomalies, often used in geophysical surveys present difficulties. The development of effective exploration techniques for the region's mineral and hydrocarbon resources will be facilitated by the research's insightful insights into underlying geological features.

The filtering techniques employed in the study have allowed for a more in-depth understanding of the geological features of the study area. By analyzing the Bouguer anomaly map and the Radially Average Power Spectrum (RAPS), the researchers were able to identify distinct characteristics of the basement and sedimentary formations.

This study provides valuable insights into the geological formations and potential for hydrocarbon exploration in the region, which could aid further exploration activities and geological studies. The use of advanced filtering techniques and derivative grids in combination with Euler deconvolution has allowed for a more detailed interpretation of the subsurface structures and anomalies in the study area. The findings of this study could have significant implications for the oil and gas industry in Nigeria and other regions with similar geological characteristics.

The significant finding of this astute erudition is the understanding and development of an improved, easier and more effective subsurface structures and anomalies from a detailed comparison of the Euler and Werner deconvolution principles. The improved interpretation and calculation are a valuable data asset for the exploration of both hydrocarbons and economic minerals.

In contribution to knowledge, this manner of approach is a milestone for the need for improved deconvolution techniques and a versatile tool for improved literature and further research in this dynamic area to reduce the magnitude of subsurface uncertainties. The promises offered to knowledge are with tremendous technical precision with an innovative approach.

Acknowledgements This research was done in collaboration with Teeiloz Nigeria Ltd, the Physics Department at the University of Calabar in Nigeria, and the Petroleum Engineering Department of Madonna University in Nigeria's College of Engineering and Technology. Federal University of Technology's Geology Department, Minna, Niger State, Nigeria. the Geosciences Department, University of Uyo, Uyo, Environmental Engineering Faculty, Cracow University of Technology, Cracow Poland and Okna Geoservices Ltd, Eket, Nigeria

Author contributions IJA and EJS were responsible for the data acquisition, interpretation, and analysis. SA provided technical guidance and expertise in the application of the Euler and Werner deconvolution techniques. AOE contributed to the literature review and interpretation of the results. INJ assisted with the data analysis and interpretation, and EDI provided critical insights and feedback throughout the project. All authors read and approved the final draft.

Data availability The data supporting the findings of this study are within the manuscript. All relevant datasets used in the research entitled "Retrospective appurtenance of Euler and Werner deconvolution contiguity for source depth excogitation of Bouguer anomalies in the Benue Trough, Nigeria" are included within the main body of the manuscript itself. These datasets contain the necessary information to replicate the results and conclusions presented in the paper. For any further inquiries regarding the data, readers are encouraged to refer to the manuscript. The authors are committed to promoting transparency and openness in scientific research, and by providing the data within the manuscript, they aim to facilitate the validation and extension of their findings by the scientific community.

Declarations

Conflict of interest The authors declare no conflict of interest.

References

Abdullahi, M., Kumar, R., & Singh, U. K. (2019). Magnetic basement depth from high-resolution aeromagnetic data of parts of lower and middle Benue Trough (Nigeria) using scaling spectral method. *Journal of African Earth Sciences, 150*, 337–345. https://doi.org/10.1016/j.jafrearsci.2018.11.006

Adegoke, J. A., & Layade, G. O. (2019). Comparative depth estimation of iron-ore deposit using the data-coordinate interpolation technique for airborne and ground magnetic survey variation. *African Journal of Science, Technology, Innovation and Development, 11*(5), 663–669. https://doi.org/10.1080/20421338.2019.1572702

Anudu, G. K., Stephenson, R. A., & Macdonald, D. I. (2014). Using high-resolution aeromagnetic data to recognise and map intra-sedimentary volcanic rocks and geological structures across the Cretaceous middle Benue Trough, Nigeria. *Journal of African Earth Sciences, 99*, 625–636. https://doi.org/10.1016/j.jafrearsci.2014.02.017

Behrendt, J. C., & Klitgord, K. D. (1980). High-sensitivity aeromagnetic survey of the U.S Atlantic continental margin. *Geophysics*. https://doi.org/10.1190/11441068

Benkhelil, J. (1989). The origin and evolution of the Cretaceous Benue Trough (Nigeria). *Journal of African Earth Sciences (and the Middle East), 82–4*, 251–282. https://doi.org/10.1016/s0899-5362(89)80028-4

Biswas, A., Parija, M., & Kumar, S. (2017). Global nonlinear optimization for the interpretation of source parameters from total gradient of gravity and magnetic anomalies caused by thin dyke. *Annals of Geophysics*. https://doi.org/10.4401/ag-7129

Egu, D. I., & Ilozobhie, A. J. (2020). Astute Expository of Vacillation Attributes of Geoseismo-Thermal Ruminative of the Turonian Maastrichtian Fika Shale in Parts of the Bornu Basin, North-Eastern Nigeria. 203606-MS paper presented at the SPE Nigeria Annual International Conference and Exhibition, 11–13 August, Nigeria. https://doi.org/10.2118/203606-ms

Emujakporue, G., Ofoha, C. C., & Kiani, I. (2018). Investigation into the basement morphology and tectonic lineament using aeromagnetic anomalies of Parts of Sokoto Basin, North Western, Nigeria. *Egyptian Journal of Petroleum, 274*, 671–681. https://doi.org/10.1016/j.ejpe.2017.10.003

Epuh, E. E., Okolie, C. J., Daramola, O. E., Ogunlade, F. S., Oyatayo, F. J., Akinnusi, S. A., & Emmanuel, E.-O.I. (2020). An integrated lineament extraction from satellite imagery and gravity anomaly maps for groundwater exploration in the Gongola Basin. *Remote Sensing Applications: Society and Environment*. https://doi.org/10.1016/j.rsase.2020.100346

Falconer, J.D. (1911). The geology and geography of northern Nigeria (London, UK: MacMillan).

Hansen, R. O., & Simmonds, M. (1993). Multiple-source Werner deconvolution. *Geophysics, 58*, 1792–1800.

Hartman, R. R., Teskey, D. J., & Friedberg, J. L. (1971). A system for rapid digital aeromagnetic interpretation. *Geophysics, 36*(5), 891–918. https://doi.org/10.1190/1.1440223

Igwe, E. O., & Okoro, A. U. (2016). Field and lithostratigraphic studies of the Eze-Aku Group in the Afikpo Synclinorium, southern Benue Trough Nigeria. *Journal of African Earth Sciences*. https://doi.org/10.1016/j.jafrearsci.2016.03.016

Ikeh, J. C., Ugwu, G. Z., & Asielue, K. (2017). Spectral depth analysis for determining the depth to basement of magnetic source rocks over Nkalagu and Igumale areas of the Lower Benue Trough, Nigeria. *International Journal of Physical Sciences, 1219*, 224–234. https://doi.org/10.5897/ijps2017.4668

Ilozobhie, A. J., & Egu, D. I. (2021). Dynamic reservoir sand characterization of an oil field in the Niger Delta from seismic and well log data. *Arabian Journal of Geosciences*. https://doi.org/10.1007/s12517-021-06542-4

Kamba, A. H., & Ahmed, S. K. (2017). Depth to basement determination using source parameter imaging (SPI) of aeromagnetic data: an application to lower sokoto basin, Northwest, Nigeria. *International Journal of Modern Applied Physics, 7*(1), 1–10.

Layade, G. O., Adebo, B. A., Olurin, O. T., & Ganiyu, O. M. (2015). Separation of Regional-Residual Anomaly Using Least Square Polynomial Fitting Method. *Journal of the Nigerian Association of Mathematical Physics, 30*, 69–180.

Layade, G. O., Edunjobi, H., Makinde, V., & Bada, B. (2020). Estimation of Depth to Bouguer Anomaly Sources Using Euler Deconvolution Techniques. *Materials and Geoenvironment, 67*(4), 185–195. https://doi.org/10.2478/rmzmag-2020-0016

Likkason, O. K. (2007). Angular Spectral analysis of aeromagnetic data over Middle Benue Trough. *Nigeria. Journal of Mining and Geology, 43*(1), 53–62.

Megwara, J. U., & Udensi, E. E. (2014). Structural analysis using aeromagnetic data: case study of parts of Southern Bida Basin Nigeria and the surrounding basement Rocks. *Earth Science Research*. https://doi.org/10.5539/esr.v3n2p27

Mickus, K. L., & Hinojosa, J. H. (2001). The complete gravity gradient tensor derived from the vertical component of gravity: a Fourier transform technique. *Journal of Applied Geophysics, 46*(3), 159–174. https://doi.org/10.1016/s0926-9851(01)00031-3

Nabighian, M. N. (1972). The analytic signal of two-dimensional magnetic bodies with polygonal cross-section: its properties and use for automated anomaly interpretation. *Geophysics, 37*(3), 507–517. https://doi.org/10.1190/1.1440276

Naidu, P. (1968). Spectrum of the potential field due to randomly distributed sources. *Geophysics, 33*(2), 337–345. https://doi.org/10.1190/1.1439933

Ngozi, A. O., Johnson, U. A., & Igwe, E. A. (2019). Spectral analysis and source parameter imaging of aeromagnetic data of Lafia and Akiri Areas, Middle Benue Trough. *Nigeria. International Journal of Physical Sciences, 14*(1), 1–14. https://doi.org/10.5897/ijps2018.4752

Nicolas, O.M. (2009): The Gravity Method. Exploration for Geothermal Resources, pp. 1–9.

Nwogwugwu, E. O., Salako, K. A., Adewumi, T., & Okwokwo, I. O. (2017). Determination of depth to basement rocks over parts of middle benue trough, North Central Nigeria, using high resolution aeromagnetic data. *Journal of Geology and Mining Research, 93*, 18–27. https://doi.org/10.5897/jgmr2017.0276

Nwosu, O. B. (2014). Determination of magnetic basement depth over parts of middle benue trough by source parameter Imaging (SPI) technique using HRAM. *International Journal of Scientific and Technology Research, 3*(1), 262–271.

Obiora, D. N., Idike, J. I., Oha, A. I., Soronnadi-Ononiwu, C. G., Okwesili, N. A., & Ossai, M. N. (2018). Investigation of magnetic anomalies of Abakaliki area, Southeastern Nigeria, using high resolution aeromagnetic data. *Journal of Geology and Mining, 10*(6), 57–71.

Ofoegbu, C. O. (1983). A review of the geology of the benue trough. *Nigeria. Journal of African Earth Sciences, 33*, 283–291. https://doi.org/10.1016/0899-5362(85)90001-6

Ofoha, C. C., Emujakporue, G., Ngwueke, M. I., & Kiani, I. (2016). Determination of magnetic basement depth over parts of sokoto basin, within Northern Nigeria, using improved source Parameter Imaging (ISPI) Technique. *World Scientific News, 50*, 266–277.

Oghuma, A. A., Obiadi, I. I., & Obiadi, C. M. (2015). 2- D Spectral analysis of aeromagnetic anomalies over parts of Montu and environs, Northeastern, Nigeria. *Journal of Earth Science and Climatic Change., 6*, 8–14. https://doi.org/10.4172/2157-7617.1000303

Olowofela, J. A., Akinyemi, O. D., Badmus, B. S., Awoyemi, M. O., Olurin, O. T., & Ganiyu, S. A. (2013). Depth estimation and source location of magnetic anomalies from a basement complex formation, using Local Wavenumber Method (LWM). *IOSR Journal of Applied Physics, 4*(2), 33–38.

Olurin, O. T., Olowofela, J. A., Akinyemi, O. D., Badmus, B. S., Idowu, O. A., & Ganiyu, S. A. (2015). Enhancement and basement depth

estimation from airborne magnetic data. *African Review of Physics, 10*(38), 303–313.

Phillips, P., Wechsler, H., Huang, J., & Rauss, P. J. (1998). The FERET database and evaluation procedure for face-recognition algorithms. *Image and Vision Computing, 16*(5), 295–306. https://doi.org/10.1016/s0262-8856(97)00070-x

Reford, M. S., & Sumner, J. S. (1964). Aeromagnetics. *Geophysics, 29*(4), 482–516. https://doi.org/10.1190/1.1439384

Reid, A. B., & Thurston, J. B. (2014). The structural index in gravity and magnetic interpretation: Errors, uses, and abuses. *Geophysics, 79*(4), J61–J66. https://doi.org/10.1190/geo2013-0235.1

Reid, A. B., Allsop, J. M., Granser, H., Millett, A. J., & Somerton, I. W. (1990). Magnetic interpretation in three dimensions using Euler deconvolution. *Geophysics, 55*(1), 80–91. https://doi.org/10.1190/1.1442774

Reid, A. B., Ebbing, J., & Webb, S. J. (2014). Avoidable Euler Errors - the use and abuse of Euler deconvolution applied to potential fields. *Geophysical Prospecting, 62*(5), 1162–1168. https://doi.org/10.1111/1365-2478.12119

Revees, C. (2005). *Aeromagnetic Surveys; Principles*. GEOSOFT: Practice and Interpretation.

Rivas, J. (2009). *Gravity and Magnetic Methods. Short course on surface exploration for geothermal resources*. United Nations University, LaGeo: Elsavador.

Roest, W. R., Verhoef, J., & Pilkington, M. (1992). Magnetic interpretation using the 3-D analytic signal. *Geophysics, 57*(1), 116–125. https://doi.org/10.1190/1.1443174

Sawuta, J. M., Ayanninuola, O. S., Udensi, E. E., & Ogwola, P. (2019). Estimation of magnetic depth to source using high resolution of aeromagnetic data of parts of upper benue trough. *North Eastern Nigeria. Science World Journal, 14*(1), 7–11.

Spector, A., & Grant, F. S. (1970a). Statistical models for interpreting aeromagnetic data. *Geophysics, 352*, 293–302. https://doi.org/10.1190/1.1440092

Spector, A., & Grant, F. S. (1970b). Statistical models for interpreting aeromagnetic data. *Geophysics, 35*(2), 293–302. https://doi.org/10.1190/1.1440092

Stavrev, P. Y. (1997). Euler deconvolution using differential similarity transformations of gravity or magnetic anomalies. *Geophysical Prospecting, 45*(2), 207–246. https://doi.org/10.1046/j.1365-2478.1997.00331.x

Telford, W. M., Geldart, L. P., & Sheriff, R. E. (1990). *Applied geophysics* (2nd ed., p. 770). Cambridge University Press.

Thompson, D. T. (1982). EULDPH: A new technique for making computer-assisted depth estimates from magnetic data. *Geophysics, 47*(1), 31–37. https://doi.org/10.1190/1.1441278

Umukoro, E. S., & Akanbi, E. S. (2014). Interpretation of aeromagnetic anomalies within Maijuju area, north central Nigeria, using Analytic signal, Euler deconvoluion and 2-d Modelling. *Nigerian Journal of Physics, 25*(2), 1.

Vanbreemen, O., Pidgeon, R., & Bowden, P. (1977). Age and isotopic studies of some Pan-African granites from North-central Nigeria. *Precambrian Research, 44*, 307–319. https://doi.org/10.1016/0301-9268(77)90001-8

Werner, S. (1953). Interpretation of magnetic anomalies at sheetlike bodies. *Geological Understanding Series, CC Arabok, 43*(6), 66–97.

Whitehead, N. and Musselman, C. (2005). Montaj Grav/Mag Interpretation: Processing, Analysis, and Visualization System for 3D Inversion of Potential Field Data for Oasis MontajTM, Tutorial and User Guide, Version 6.1, Geosoft Inc., Toronto, ON, Canada M5J 1A7.

Wright, J.B. (1976). Origin of the Benue trough- a critical review, in C.A., Kogbe (2), Geology of Nigeria, (Lagos, Nigeria: Elizabethan Publication Company), 309–317.

Zahra, H. S., & Oweis, H. T. (2016). Application of high-pass filtering techniques on gravity and magnetic data of the eastern Qattara depression area, western desert. *Egypt. NRIAG Journal of Astronomy and Geophysics, 5*(1), 106–123. https://doi.org/10.1016/j.nrjag.2016.01.005

Terms and Conditions

Springer Nature journal content, brought to you courtesy of Springer Nature Customer Service Center GmbH (“Springer Nature”).
Springer Nature supports a reasonable amount of sharing of research papers by authors, subscribers and authorised users (“Users”), for small-scale personal, non-commercial use provided that all copyright, trade and service marks and other proprietary notices are maintained. By accessing, sharing, receiving or otherwise using the Springer Nature journal content you agree to these terms of use (“Terms”). For these purposes, Springer Nature considers academic use (by researchers and students) to be non-commercial.
These Terms are supplementary and will apply in addition to any applicable website terms and conditions, a relevant site licence or a personal subscription. These Terms will prevail over any conflict or ambiguity with regards to the relevant terms, a site licence or a personal subscription (to the extent of the conflict or ambiguity only). For Creative Commons-licensed articles, the terms of the Creative Commons license used will apply.
We collect and use personal data to provide access to the Springer Nature journal content. We may also use these personal data internally within ResearchGate and Springer Nature and as agreed share it, in an anonymised way, for purposes of tracking, analysis and reporting. We will not otherwise disclose your personal data outside the ResearchGate or the Springer Nature group of companies unless we have your permission as detailed in the Privacy Policy.
While Users may use the Springer Nature journal content for small scale, personal non-commercial use, it is important to note that Users may not:

1. use such content for the purpose of providing other users with access on a regular or large scale basis or as a means to circumvent access control;
2. use such content where to do so would be considered a criminal or statutory offence in any jurisdiction, or gives rise to civil liability, or is otherwise unlawful;
3. falsely or misleadingly imply or suggest endorsement, approval , sponsorship, or association unless explicitly agreed to by Springer Nature in writing;
4. use bots or other automated methods to access the content or redirect messages
5. override any security feature or exclusionary protocol; or
6. share the content in order to create substitute for Springer Nature products or services or a systematic database of Springer Nature journal content.

In line with the restriction against commercial use, Springer Nature does not permit the creation of a product or service that creates revenue, royalties, rent or income from our content or its inclusion as part of a paid for service or for other commercial gain. Springer Nature journal content cannot be used for inter-library loans and librarians may not upload Springer Nature journal content on a large scale into their, or any other, institutional repository.
These terms of use are reviewed regularly and may be amended at any time. Springer Nature is not obligated to publish any information or content on this website and may remove it or features or functionality at our sole discretion, at any time with or without notice. Springer Nature may revoke this licence to you at any time and remove access to any copies of the Springer Nature journal content which have been saved.
To the fullest extent permitted by law, Springer Nature makes no warranties, representations or guarantees to Users, either express or implied with respect to the Springer nature journal content and all parties disclaim and waive any implied warranties or warranties imposed by law, including merchantability or fitness for any particular purpose.
Please note that these rights do not automatically extend to content, data or other material published by Springer Nature that may be licensed from third parties.
If you would like to use or distribute our Springer Nature journal content to a wider audience or on a regular basis or in any other manner not expressly permitted by these Terms, please contact Springer Nature at

onlineservice@springernature.com